10.1071/CH20176_AC

Australian Journal of Chemistry 2020, 73(12), 1260-1270

SUPPLEMENTARY MATERIAL

Photochemically Induced Solid State Dimerisation of Resveratrol Analogues: A Greener Synthetic Process‡

Basil Danylec,[A] Eva M. Campi,[A] Craig M. Forsyth,[A] Reinhard I Boysen,[A] and Milton T. W. Hearn[A,B]

[A]School of Chemistry, Monash University, Clayton, Vic. 3800, Australia.

[B]Corresponding author. Email: milton.hearn@monash.edu

‡ This paper is dedicated to the memory of our friend and long-time collaborator, W Roy Jackson AM, whose compassion, unwavering commitment to scientific excellence and generosity of spirit were beacons to all who were privileged to know him.

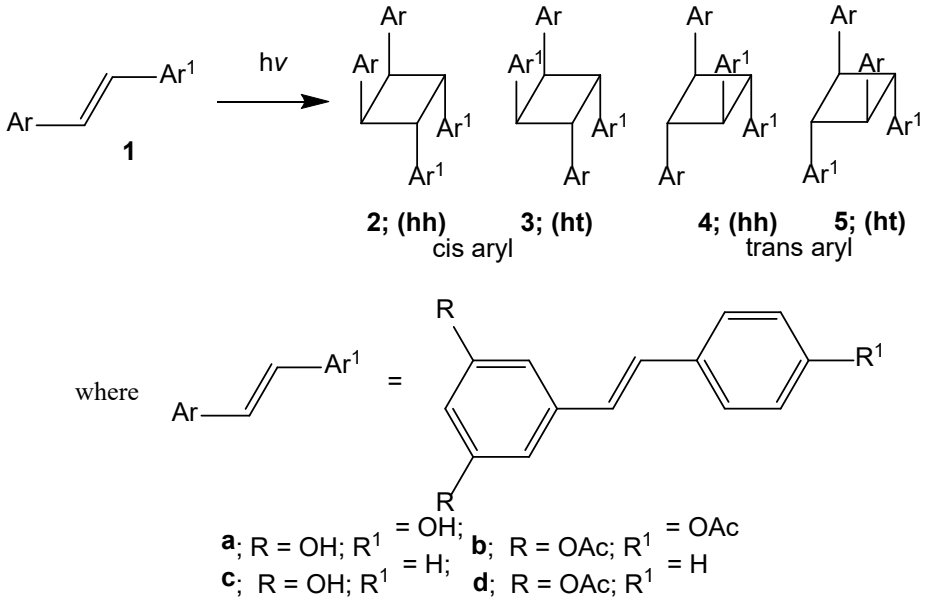

Fig. S1 **S**tructures of the possible regio- and stereo-isomeric cyclobutane dimeric products that could be generated from the UV irradiation of resveratrol and analogues in the solid state.

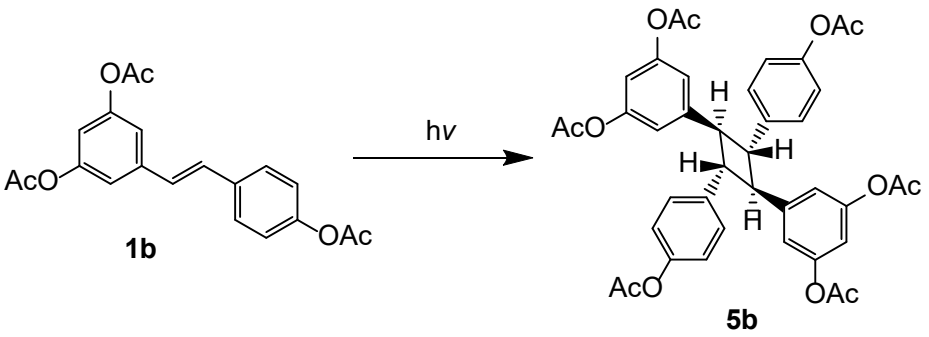

Fig. S2 UV irradiation of triacetyl resveratrol **1b** to give the cyclobutane dimer **5b**.

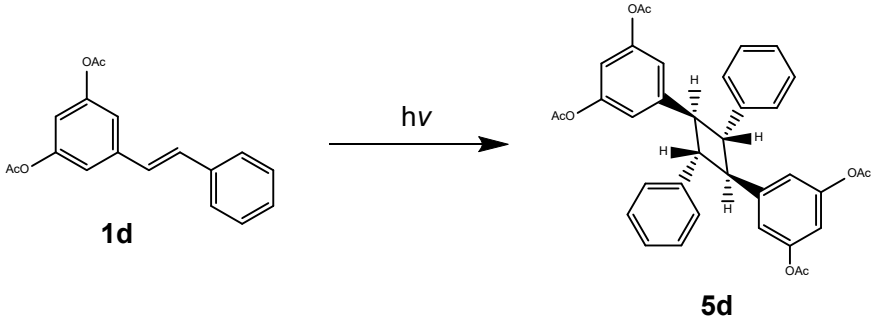

Fig. S3 UV irradiation of 3,5-diacetoxy (*E*)-stilbene (**1d**) to give cyclobutane dimer (**5d**).

Nuclear Magnetic Resonance Spectral Analysis

Nuclear magnetic resonance spectra were recorded at 400 MHz (^{1}H NMR) or 100 MHz (^{13}C NMR) with a Bruker DRX400 spectrometer. The NMR spectra refer to solutions in $CDCl_3$, CD_3OD or CD_3CN with residual solvent peak used as an internal standard for ^{1}H spectra and the solvent peak used as an internal reference in ^{13}C spectra. ^{1}H and ^{13}C NMR spectrum of pure cyclobutane **5b**, ^{1}H NMR spectra of various product fractions after UV irradiation of **1b**, ^{1}H NMR spectra of pure cyclobutane **5d,** ^{1}H and ^{13}C NMR spectra of the phenolic cyclobutanes **5a** and **5c.**

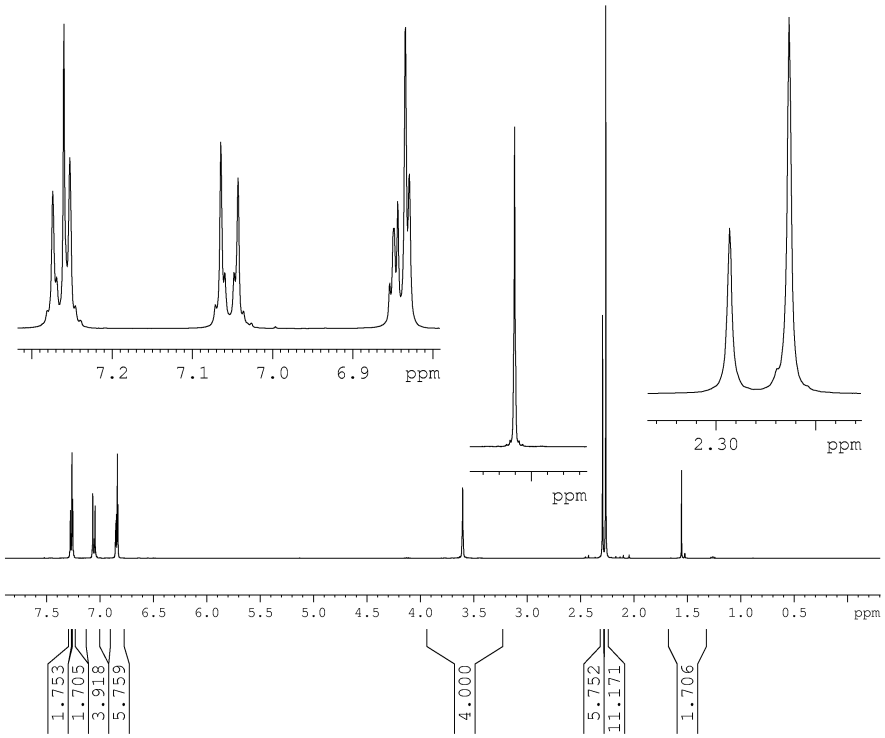

Fig. S4 ^{1}H NMR spectrum of pure triacetyl resveratrol cyclobutane dimer (**5b**; R, R′ = OAc)

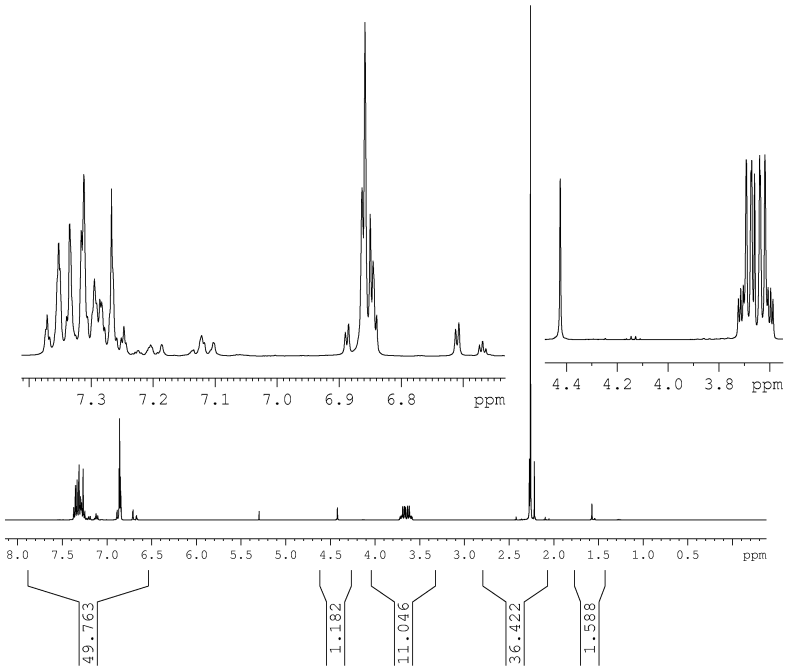

Fig. S5 ^{1}H NMR spectrum of the crude product after photodimerization of (**1d**; R = OH; R′ = H)

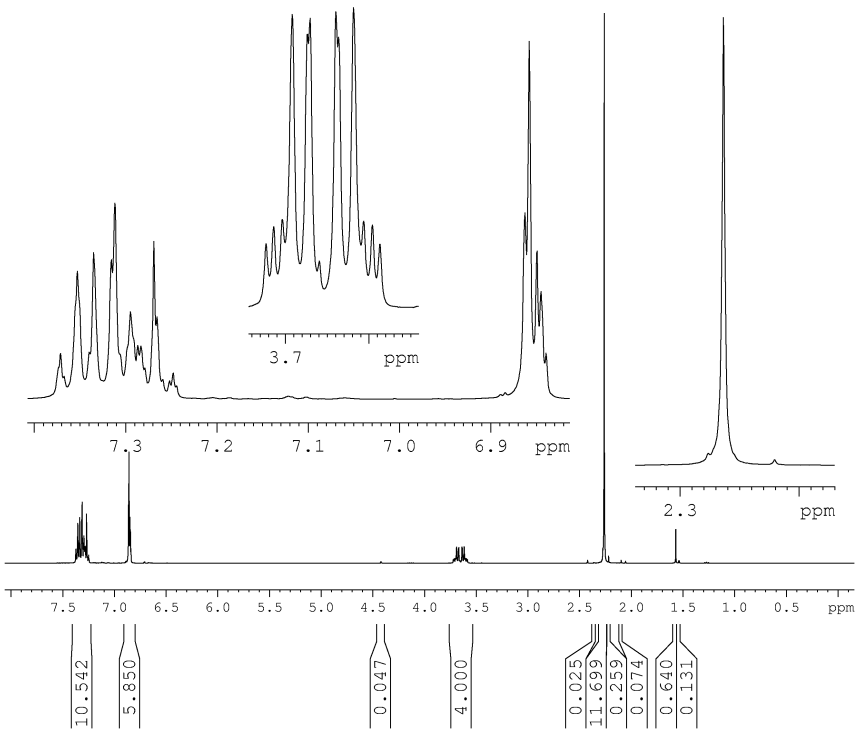

Fig. S6 ^{1}H NMR spectrum of chromatographed product, 99% pure (**5d**; R = OAc; R′ = H)

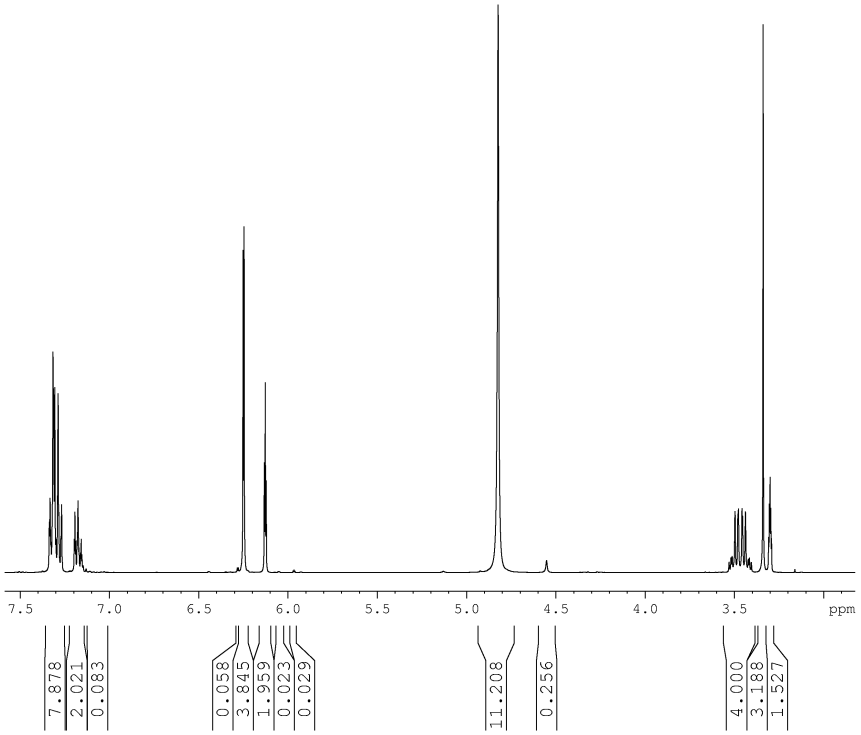

Fig. S7 ^{1}H NMR spectrum of the phenolic cyclobutane (**5c**; R = OH; R′ = H)

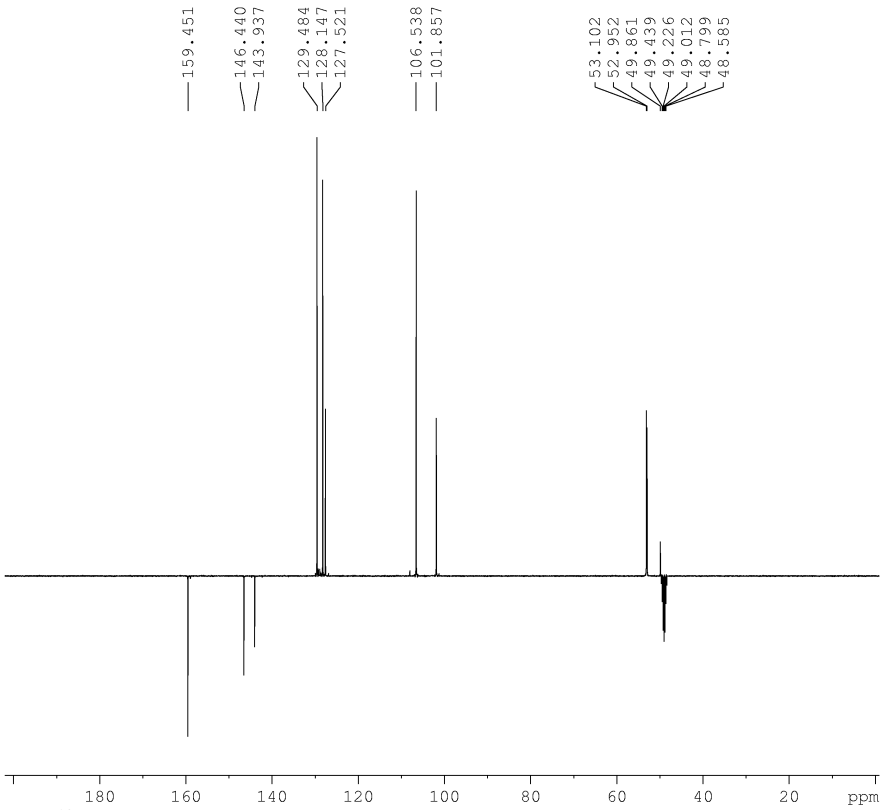

Fig. S8 ^{13}C NMR spectrum of the phenolic cyclobutane (**5c**; R = OH; R′ = H)

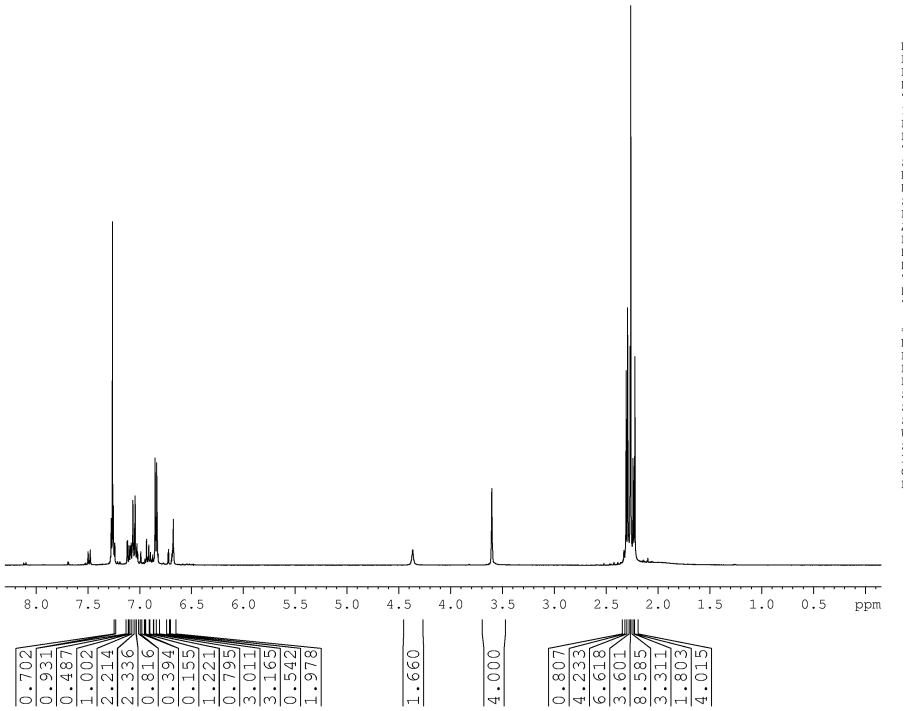

Fig. S9 ^{1}H NMR spectrum of irradiated triacetyl resveratrol (**1b**; R, R′ = OAc) after 83 h

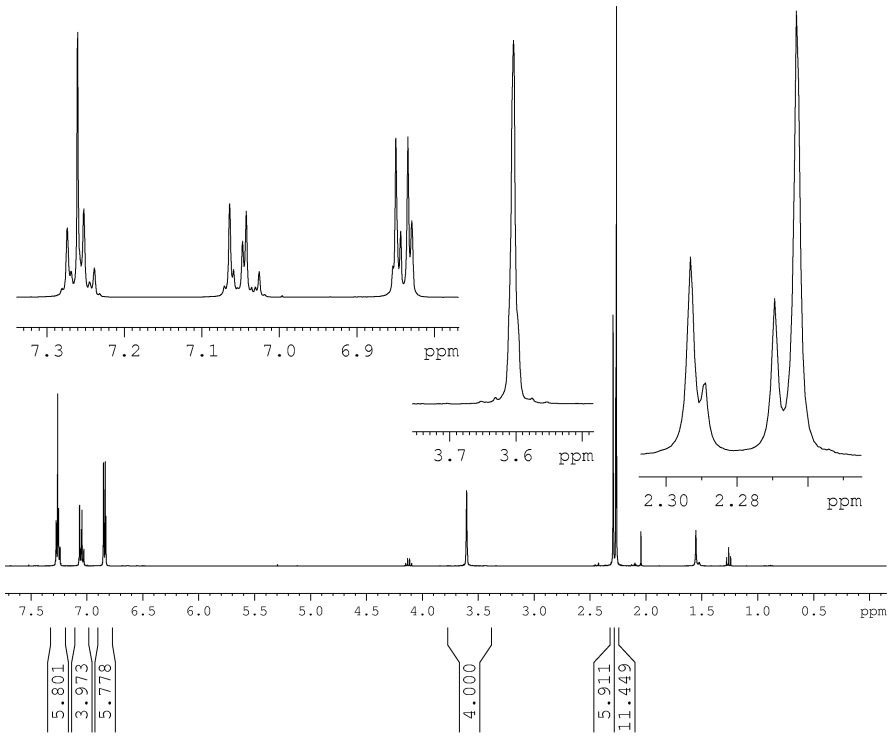

Fig. S10 ^{1}H NMR spectrum of fractions 22-27 from column chromatography after low power irradiation of triacetyl resveratrol (**1b**; R, R′ = OAc)

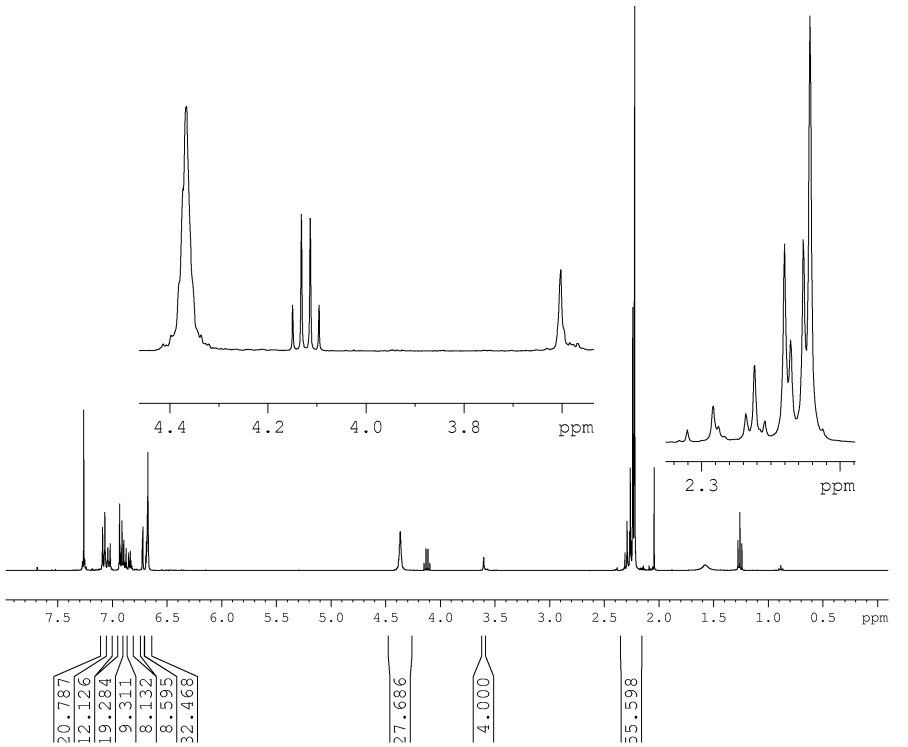

Fig. S11 ^{1}H NMR spectrum of fractions 30-34 from column chromatography after low power irradiation of triacetyl resveratrol (**1b**; R, R′ = OAc)

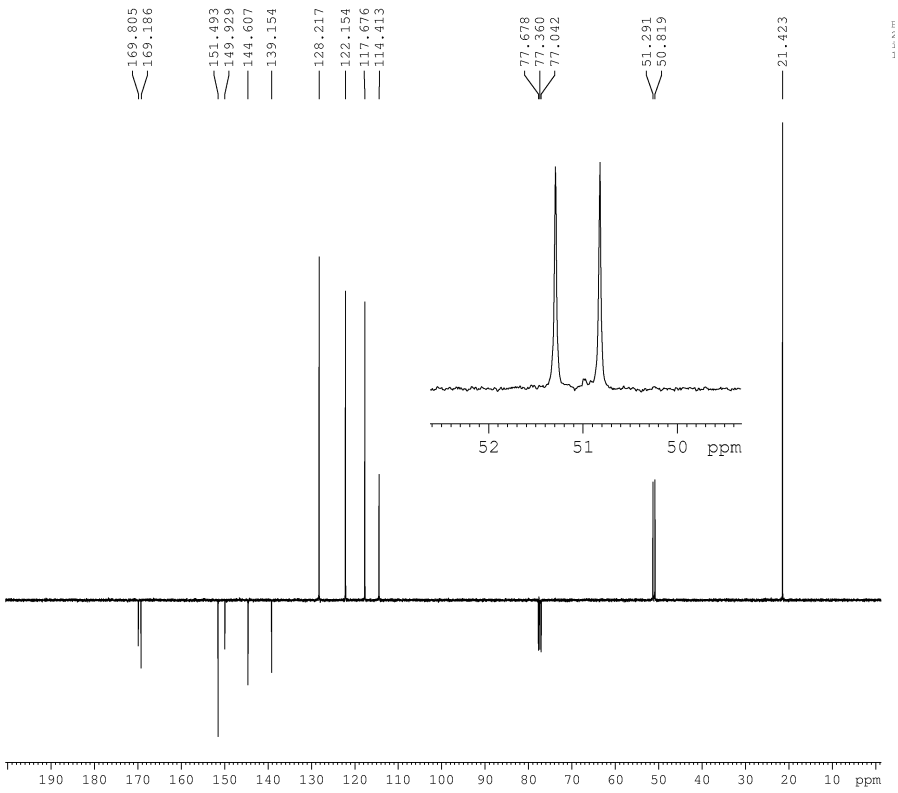

Fig. S12 ^{13}C NMR spectrum of pure triacetyl resveratrol cyclobutane dimer (**5b**; R, R′ = OAc)

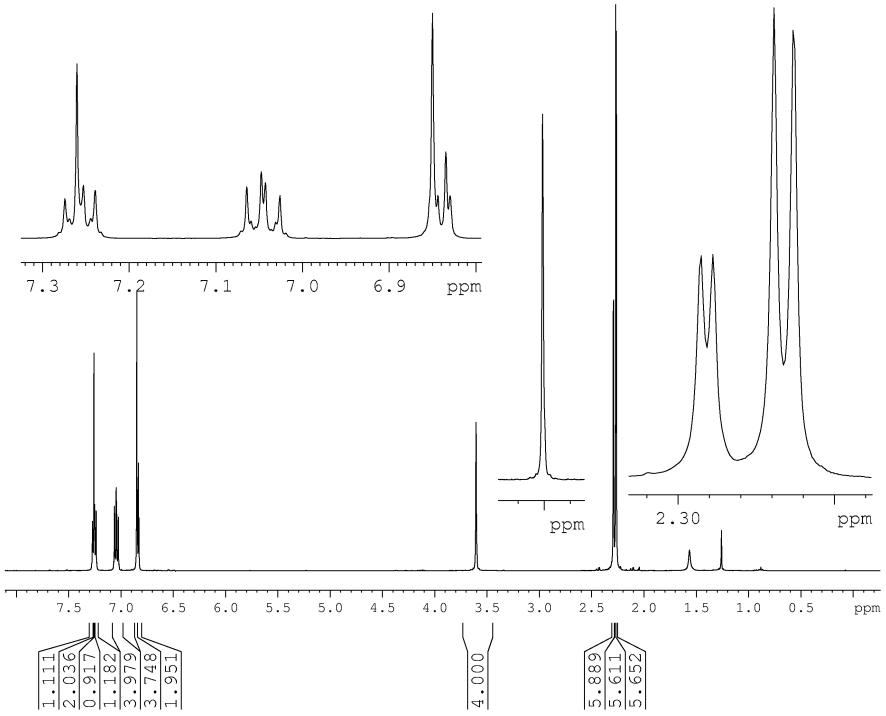

Fig. S13 ^{1}H NMR of solid recovered from filtrate of recrystallised fraction 22-27 from column chromatography after low power irradiation of triacetyl resveratrol (**1b**; R, R′ = OAc)

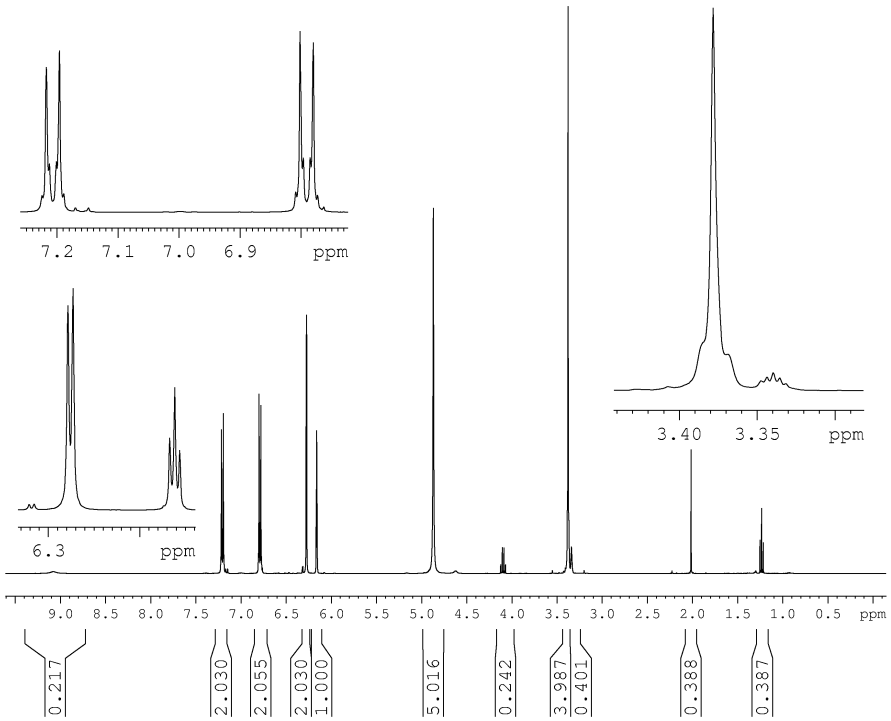

Fig. S14 ^{1}H NMR spectrum of resveratrol dimer (**5a**; R, R′ = OH) in CD_3OD

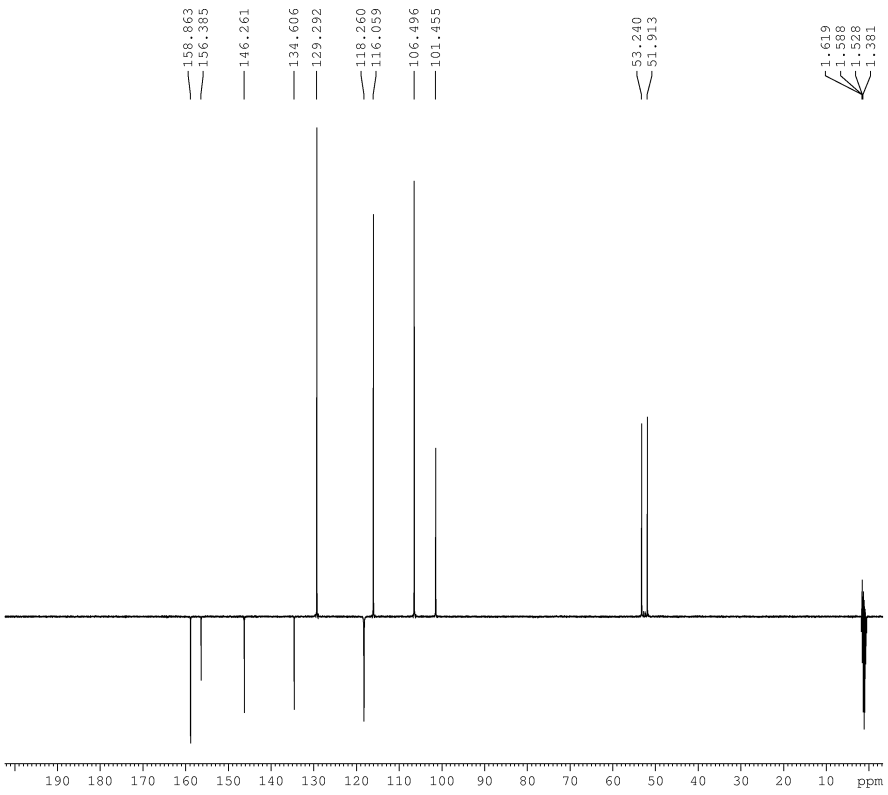

Fig. S15 ^{13}C NMR spectrum of resveratrol dimer (**5a**; R, R′ = OH) in CD_3CN

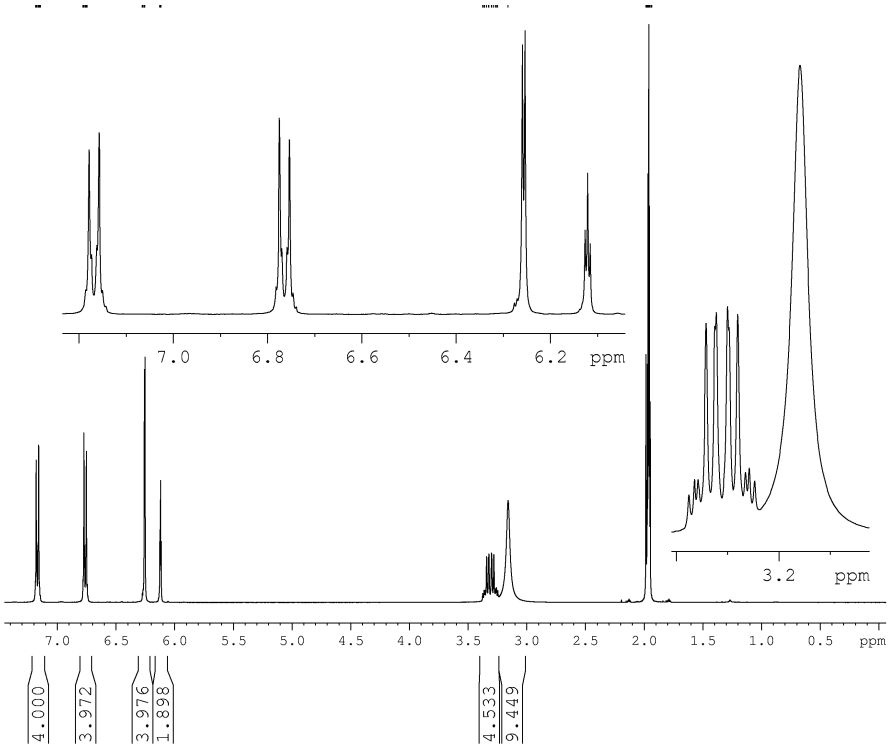

Fig. S16 ^{1}H NMR spectrum of resveratrol dimer (**5a**; R, R′ = OH) in CD_3CN after D_2O exchange

LC ESI-MS Analysis

Sample preparation. The resveratrol dimer was dissolved at a concentration of 10 μM in 0.1 M Formic acid (FA) and directly analysed by LC-MS.

LC MS instrumentation. Analyses was performed on a 1200 series Nano LC instrument (Agilent Technologies, Waldbronn, Germany) coupled to a MicroTOFq quadrupole TOF mass spectrometer (Bruker Daltonics, Bremen, Germany).

Data Acquisition and processing. Samples were analysed by LC-MS/MS by separation with a 30 minute gradient using a C18 Zorbax, 75 μm x 15 cm i.d., 100 Å pore size, reversed-phase nano column (Agilent Technologies) with 95% eluent A (0.1% formic acid) to 70% eluent B (80% (v/v) acetonitrile 0.1% formic acid), at a flow rate of 300 nL/minute The eluate was nebulised and ionised using the Bruker nanoSI source with a capillary voltage of 4000 V in the negative and positive ion mode. Analytes were selected for MS/MS analysis in the autoMS^n mode based on peak intensity selecting one precursor ion and active exclusion released after 2 minutes. Prior to analysis, the qTOF mass spectrometer was calibrated using an ESI-L low concentration tuning mix G1969-85000 from Agilent Technologies. The spectra were extracted and deconvoluted using Data Analysis software version 3.4 (Bruker Daltonics).

The LC ESI MS analysis allowed detection of the resveratrol dimer in the positive ion mode as the singly charged $[M+H]^+$ ion with *m/z* = 457.2 (expected *m/z* = 457.164566) and the

doubly charged $[M+2H]^{2+}$ ion with *m/z* = 229.1 (expected *m/z* = 229.085921) and in the negative ion mode as the singly charged $[M-H]^-$ ion with *m/z* = 455.1 (expected *m/z* = 455.150014) and the doubly charged $[M-2H]^{2-}$ ion with *m/z* = 227.1 (expected *m/z* = 227.071369).

Whilst no ESI (-) MS/MS spectrum could be obtained, the ESI (+) MS/MS spectrum of the resveratrol dimer is characterized by a small number of ion fragments diagnostic of the resveratrol monomer structure (Fig. S17) with *m/z* = 91.1, *m/z* = 107.1, *m/z* = 135.0 and *m/z* = 165.1.[S1, S2] The suggested fragmentation pathways of the resveratrol dimer precursor ion (*m/z* = 457) in the positive ion mode are depicted in Fig. S18 and is thought to occur *via* the resveratrol monomer ion (*m/z* = 229).

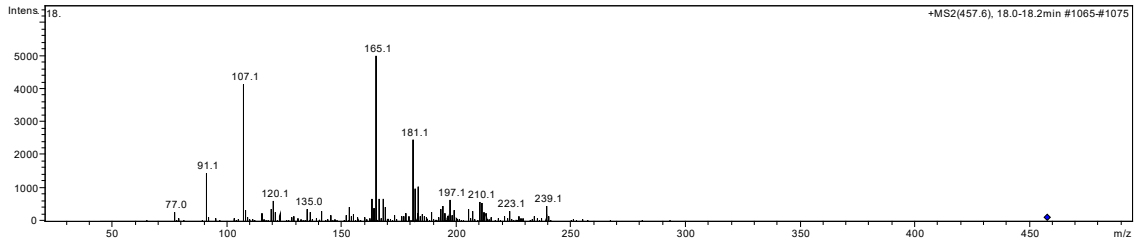

Fig. S17 ESI (+) MS/MS spectrum of the resveratrol dimer at *m/z* = 457 obtained at the time window from 18.0-18.2 min in the LC MS run (sample injection 1 μL).

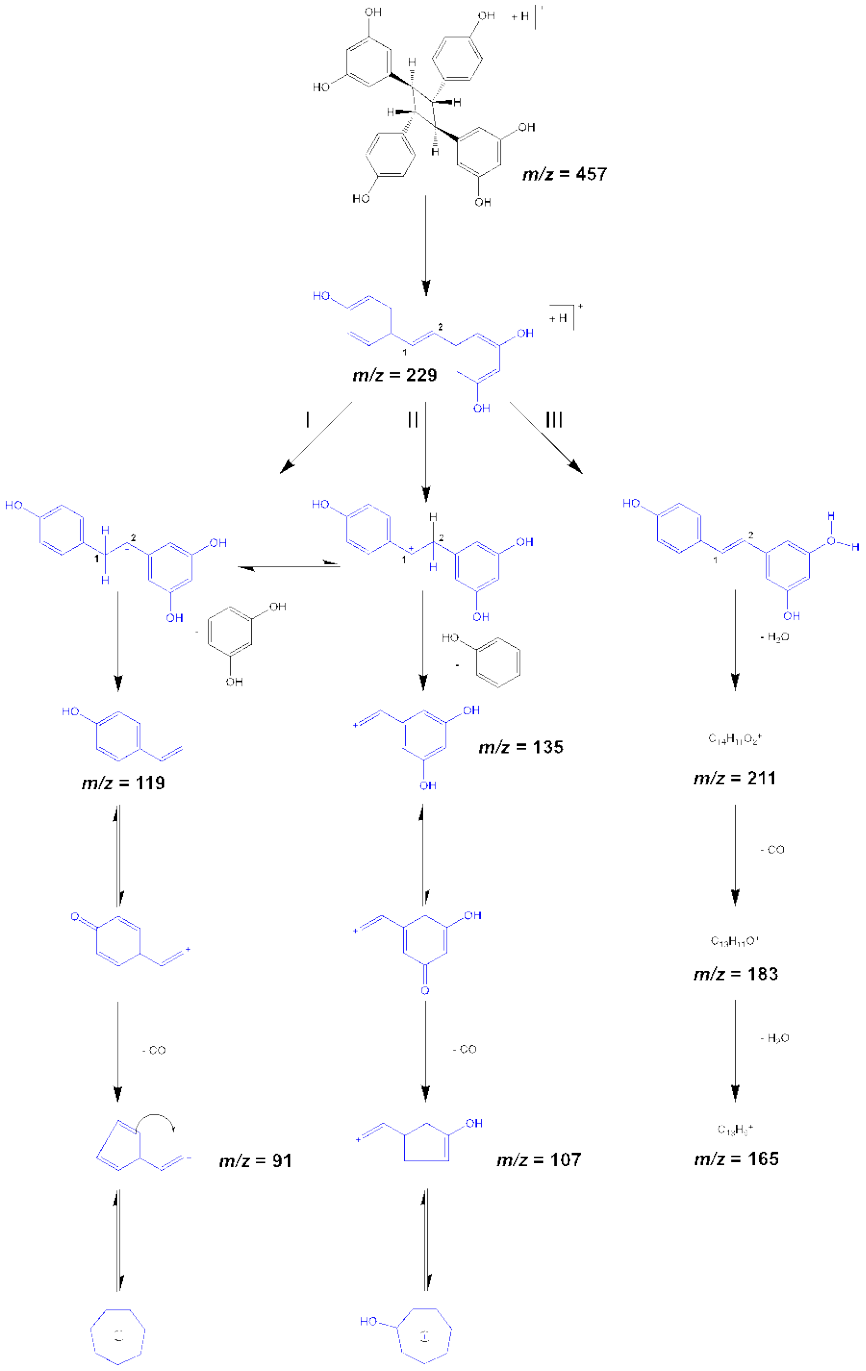

Fig. S18 MS/MS fragmentation pathways of resveratrol dimer in the positive ion mode.

Three different protonation sites can be suggested for the protonated molecular ion of the resveratrol monomer.[S3] Two protonation sites are located at the stilbene double bond, resulting in two possible fragmentation pathways, depending on the regiochemistry of proton addition to the double bond. When carbon 1 is protonated (Fig. S18: pathway I), the fragmentation of the $[M+H]^+$ species leads to the formation of ions at *m/z* = 119, through the loss of the resorcinol group, followed by CO elimination resulting in the product ion at *m/z* = 91. When carbon 2 is

protonated (Fig. S18: pathway II), the loss of phenol gives rise to the formation of the product ion at *m/z* = 135, which is followed by the formation of the product ion at *m/z* = 107 due to the neutral loss of CO. The third type of protonation site, located on the hydroxyl group of either phenol or resorcinol rings (Fig. S18: pathway III), could give rise to the product ion at *m/z* = 211, which corresponds to the neutral loss of water from the precursor ion, followed by the neutral loss of CO, resulting in the product ion at *m/z* = 183, and again the neutral loss of water, resulting in the product ion at *m/z* = 165.

Packing diagrams for *trans*-resveratrol 1a and triacetyl *trans*-resveratrol 1b:

A revised crystal structure for *trans*-resveratrol **1a** has been reported by Zarychta et al[S4] in which **1a** packs as parallel molecules in a classic herringbone fashion (Fig. S19a) whereas the O-acetyl analogue **1b** reported by Tang et al[S5] packs as twisted head-to-tail pairs (related by a crystallographic two-fold axis) (Fig. S19b).

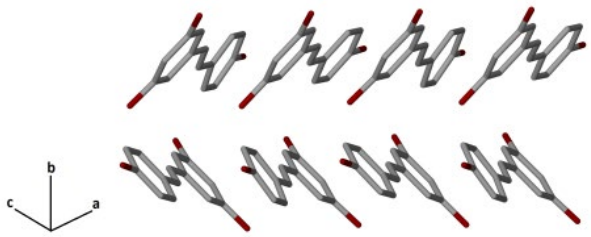

Fig. S19a Packing diagram, with axes labelled, for *trans*-resveratrol **1a** showing parallel molecules in a classic herringbone fashion[S4]

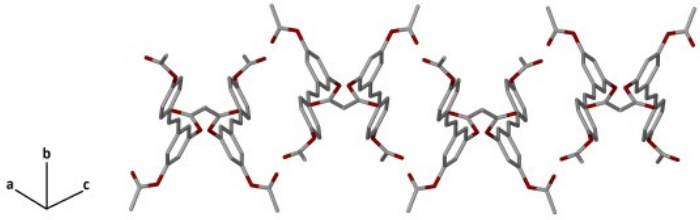

Fig. S19b Packing diagram, with axes labelled, for triacetyl *trans*-resveratrol **1b** showing twisted head-to-tail pairs (related by a crystallographic two-fold axis)[S5]

References

[S1] M.N. Bravo, R. Feliciano, S. Silva, A.V. Coelho, L. Vilas Boas, M.R. Bronze, *J. Food Compos. Anal.* **2008**, *21*, 634. https://doi.org/10.1016/j.jfca.2008.04.007.

[S2] D. Callemien, V. Jerkovic, R. Rozenberg, S. Collin, *J. Agric. Food Chem.* **2005**, *53*, 424. https://doi.org/10.1021/jf040179n.

[S3] L. Di Donna, F. Mazzotti, H. Benabdelkamel, B. Gabriele, P. Plastina, G. Sindona, *Anal. Chem.* **2009**, *81*, 8603. https://doi.org/10.1021/ac9015243.

[S4] B. Zarychta, C. G. Gianopoulos, A. A. Pinkerton, *Bioorg. Med. Chem. Lett*. **2016**, *26*, 1416

[S5] L. Tang, D. Dai, Y. Gong, J. Zhong, *Acta Cryst, Sect. E*, **2011**, *67*, o3129